Section A-Research paper
ISSN 2063-5346

HQSAR, CoMFA and CoMSIA analysis of benzimidazole derivatives as anti-hypertensive agents

Deepti Mishra, Jitendra Sainy*, Rajesh Sharma

School of Pharmacy, Devi Ahilya Vishwavidyalaya, Indore-452001

***Corresponding author**

jsainy24@gmail.com
School of Pharmacy
Devi Ahilya Vishwavidyalaya, Indore (India)-452001

Abstract- The incidence rate of hypertension continues a phenomenal rise and so, there is an ever-increasing demand for the discovery of novel therapeutic agents that have increased efficacy and decreased adverse effects. In these circumstances, benzimidazole was chosen as a potential lead structure and subjected to hologram quantitative structure–activity relationship (HQSAR), comparative molecular field analysis (CoMFA), and comparative molecular similarity indices analysis (CoMSIA). In general, the findings of the QSAR analysis indicate that the LOO cross-validated q2 and r2 values of the HQSAR, CoMFA, and CoMSIA models are respectively 0.983, 0.178, and 0.416, and 0.991, 0.996, and 0.996. HQSAR found that the hydrogen bond donor and acceptor play a big role in how well benzimidazole derivatives work against high blood pressure.

1. Introduction

Cardiovascular diseases are a serious health problem worldwide. Uncontrolled blood pressure is one of the main risk factors for cardiovascular diseases (CVDs) such as heart attacks and stroke, and are responsible for one-third of total deaths in India. [2]

Hypertension, along with pre-hypertension and other hazardously high blood pressure, is responsible for 8·5 million deaths from stroke, ischaemic heart disease, other vascular diseases, and renal disease worldwide. Global scenario reveals that only cardiovascular disease accounts one third of deaths of total and more than half cases among these complications are due to hypertension. It is a major cause of premature death worldwide [1].

Hypertension is defined as increased systolic pressure, diastolic pressure, or both [3] The first systolic represents pressure in blood vessels when the heart contracts or beats and second

diastolic represents pressure in the vessels when the heart rests between beats. High blood pressure is said to be present if it is persistently at or above 140/90 mmHg.

The incidence rate of hypertension continues a phenomenal rise [1] and so, there is a growing need to identify novel therapeutic agents with improved efficacy and reduced side effects.

More people die each year from cardiovascular diseases than from any other cause. Over three quarters of heart disease and stroke-related deaths occur in low-income and middle-income countries.

An estimated 1.4 billion people worldwide have high blood pressure, but just 14% have it under control. However, cost-effective treatment options do exist. More than 700 million people with untreated hypertension, nearly half these people did not know they had hypertension. In 2019, over one billion people with hypertension (82% of all people with hypertension in the world) lived in low- and middle-income countries.[2]

According to WHO the number of people aged 30–79 years with hypertension doubled from 1990 to 2019, from 331 (95% credible interval 306–359) million women and 317 (292–344) million men in 1990 to 626 (584–668) million women and 652 (604–698) million men in 2019, despite stable global age-standardised prevalence [1].

The development of anti-hypertensive drugs represents one of the most important advances in therapeutics both in the control or cure and treatment of blood pressure complications of other therapeutic modalities such as cardiovascular disease [5].

Benzimidazole nucleus is the most important building block for several of compounds that play important roles in the physiological function of various biologically as well as physiologically important molecules [17].

For more than twenty years, computational methodologies and QSAR analysis have been gained popularity in designing novel drug molecules. In the present work we have been utilizing hologram quantitative structure–activity relationship (HQSAR), comparative molecular field analysis (CoMFA), and comparative molecular similarity indices analysis (CoMSIA) [7-12] techniques for exploring structural constraints around the benzimidazole ring, which may be helpful in designing new benzimidazole classes of anti hypertensive drugs.

2. Materials and methods

2.1 Dataset-

Total 52 structurally different benzimidazole derivatives in the dataset, which have been shown to have activity against the hypertension, were used for 2D and 3D QSAR modelling. The IC_{50} values, which represent the inhibitor concentration (in M) that results in 50% inhibition, were converted into pIC_{50} (log IC_{50}) values and used as a dependent variable in HQSAR, CoMFA, and CoMSIA analysis. According to the substitution at the R, R1, R2 and R3 position on benzimidazole ring, 52 benzimidazole derivatives were randomly divided into the training set (35 compounds) and test set (17 compounds). The test compounds were selected considering the structural diversity and wide range of activity within the dataset. Chemical structures and their biological activities are represented in table 1.

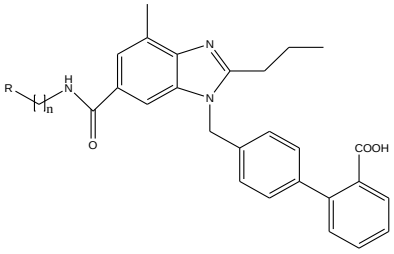

6a-6i

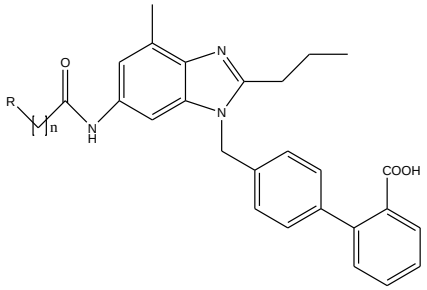

11b-11g, 12

S.no.	Name	n	R	pIC_{50}
1	11b	0	Ethyl	9.397
2	11c	0	n-Propyl	9.522
3	11d	0	Phenyl	8.408
4	11e	0	4-Methylphenyl	8.309
5	11f	1	Phenyl	8.920
6	11g	2	Phenyl	10
7	12	0	Methoxy	9.154
8	6b	0	n-Butyl	7.886
9	6d	0	1-Piperidinyl	7.698

10	6e	0	4-Methylphynyl	7.408
11	6f	2	Phenyl	8.522
12	6g	2	4-Morpholinyl	7.958
13	6i	3	4-Morpholinyl	8

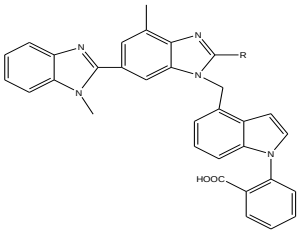

1a-1e

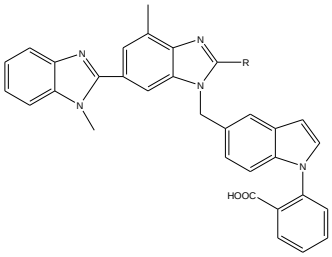

2a-2e

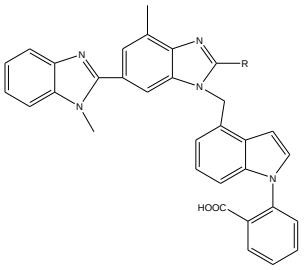

3

S.no.	Name	R	pIC_{50}
14	1a	Me	8.127
15	1b	Et	8.737
16	1c	n-Pr	9.443
17	1d	n-Bu	8.583
18	1e	n-Pentyl	7.946
19	2a	Methyl	8.083
20	2b	Ethyl	7.884
21	2c	n-Propyl	8.424
22	2d	n-Butyl	8.651
23	2e	n-Pentyl	9.036
24	3	/	8.469

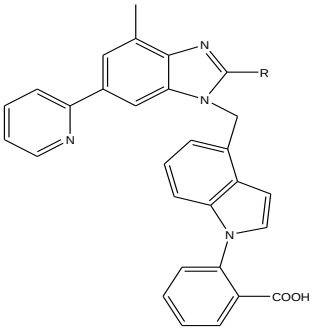

4a-4c

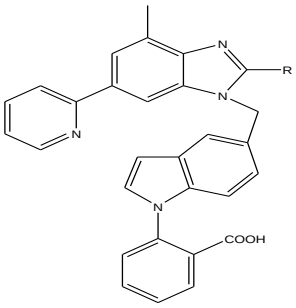

5a-5c

S.no.	Name	R	pIC_{50}
25	4a	Ethyl	8.449
26	4b	n-Propyl	8.327
27	4c	n-Butyl	8.249
28	5a	Ethyl	8.931
29	5b	n-Propyl	8.485
30	5c	n-Butyl	8.251

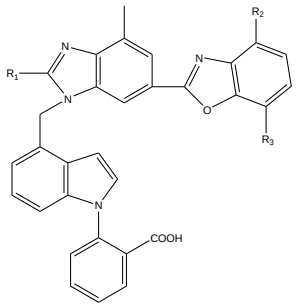

1A-1F

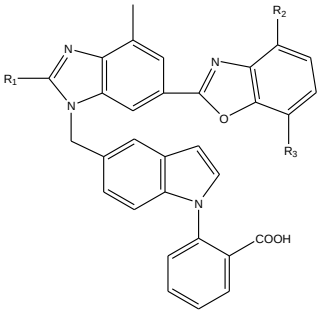

2A-2F

S.no.	Name	R1	R2	R3	pIC_{50}
31	1A	Ethyl	Methyl	H	7.987
32	1B	n-Propyl	Methyl	H	8.397
33	1C	n-Butyl	Methyl	H	8.004
34	1D	Ethyl	H	Methyl	7.917

35	1E	n-Propyl	H	Methyl	8.275
36	1F	n-Butyl	H	Methyl	7.978
37	2A	Ethyl	Methyl	H	7.920
38	2B	n-Propyl	Methyl	H	8.356
39	2C	n-Butyl	Methyl	H	7.970
40	2D	Ethyl	H	Methyl	7.866
41	2E	n-Propyl	H	Methyl	8.251
42	2F	n-Butyl	H	Methyl	8.013

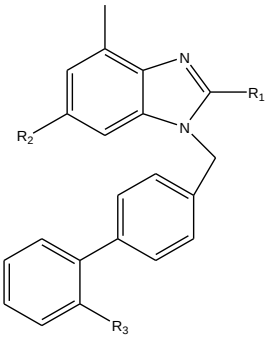

1b-1i, 2a-2b

S.no	Compound name	R1	R2	R3	pIC_{50}
43	1b	$-CH_2CH_2CF_3$	-COOH	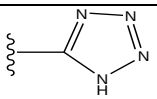	8.148
44	1c	$-CH_2CH_2CF_3$	-COOH	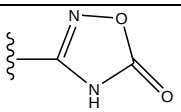	8.136
45	1d	$-CH_2CH_2CF_3$	$-CON(CH_3)_2$	-COOH	8.318
46	1e	$-CH_2CH_2CF_3$	$-CON(CH_2CH_3)_2$	-COOH	8.267
47	1f	$-CH_2CH_2CF_3$	$-CONH(CH_2)_2C_6H_5$	-COOH	8.283
48	1g	$-CH_2CH_2CF_3$	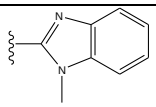	-COOH	9.096

49	1h	$-CH_2CH_2CF_3$	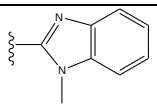	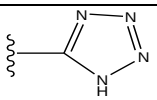	8.481
50	1i	$-CH_2CH_2CF_3$	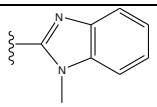	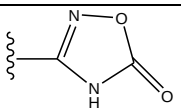	8.346
51	2a	$-CH_2CH_2CH_2F$	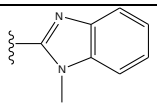	-COOH	8.638
52	2b	$-CH_2CH_2CH_2F$	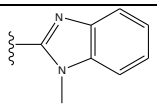	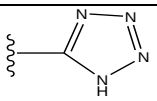	8.251

2.2 Molecular modelling -

The three dimensional structures of benzimidazole were built using the sketch module of SYBYL-X 2.1 and the energy minimized through MMFF94 (Merck molecular force field 94); the Gasteiger–Huckle charge was then added by SYBYL-X 2.1.

2.3 Molecular alignment for 3D-QSAR analysis-

One of the most crucial and sensitive 3D-QSAR parameters is molecular alignment. Aligning molecules correctly was necessary for the CoMFA and CoMSIA to produce reliable 3D-QSAR models.The molecules in the dataset were aligned using the maximum common substructure method. In dataset's most active compound, compound 6 (IC_{50} =0.1, pIC_{50} =10), served as a template for aligning the molecules in the training and test sets.

The DATABASE ALIGN option of SYBYL-X 2.1 was used to align the molecules over the template molecule by rotation and translation so as to minimize the root mean square deviation (RMSD) between atoms in the template and the corresponding atoms in the analogues. The template compound 6 with maximum common substructure and aligned molecules are shown in Figure 1

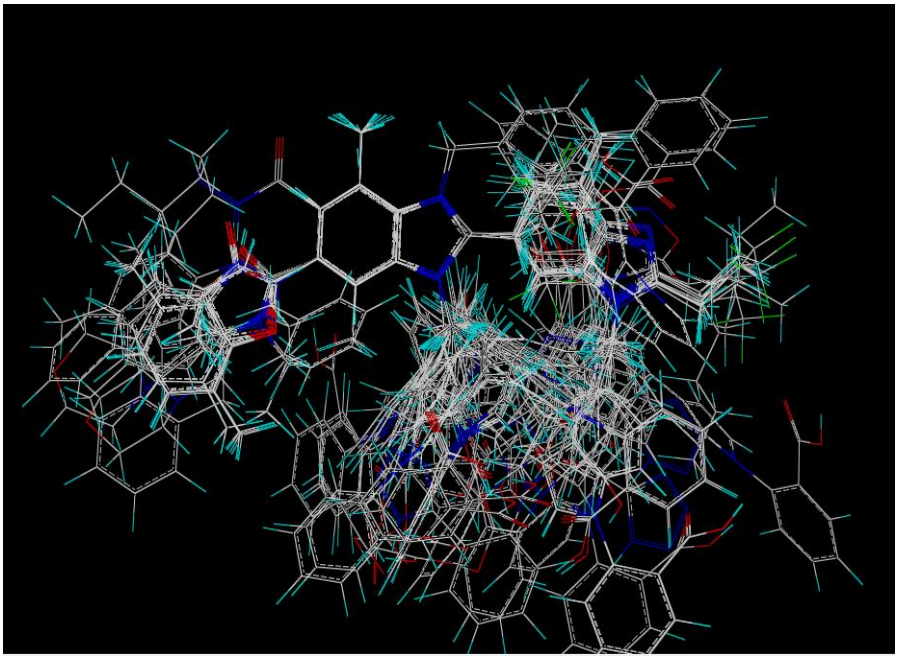

Figure 1 Molecular alignment of all molecules over template molecule.

2.4 Calculation of hologram quantitative structure–activity relationship descriptors

HQSAR is an approach that may be used to determine the relationship that exists between the structure of a molecule and the biological activity of that substance [8]. The ability to generate molecular alignment and conformational specification without the necessity for a 3D structure is one of the benefits of this technique. Other advantages include the choice to calculate or measure physicochemical descriptors, as well as the flexibility to select those characteristics.

In HQSAR, each molecule in the dataset is broken down into all of the possible structural fragments, and the user is able to choose a minimum and maximum for the number of atoms in each fragment. An individual integer is assigned to each one of the unique fragments. This integer corresponds to a bin-in-an-integer array that has a predetermined holographic length (HL), which is commonly between 50 and 500. A molecular hologram is formed as a result of the arrangement of these pieces when they are put together. The most effective HQSAR model was created by first sorting through the 12 default HL values, which were a collection of 12 prime integers (53, 59, 61, 71, 83, 97, 151, 199, 257, 307, 353 and 401). Techniques such as traditional partial least square (PLS) analysis, leave-one-out (LOO) cross-validation, and LOO without cross-validation are utilised in order to estimate the amount of components that will provide the best feasible predictive model. During the process of fragment creation, the same fragments are repeatedly hashed to the same bin, which causes an increase in the

corresponding occupancy of that bin. In this work, all 21 HQSAR studies were performed by setting values of hologram length with all 153 odd integers ranging from 97 to 401. This was done in order to reduce the possibility of collisions between identical or similar fragments . The development of HQSAR models may be affected by the hologram length, fragment size, and fragment distinction factors. When developing the HQSAR model, a number of different permutations of these factors were considered and taken into account.

2.5 Calculation of comparative molecular field analysis descriptors

Both the CoMFA and the CoMSIA models were created with the help of the molecular modelling programme known as SYBYL-X 2.1 [12]. For the purposes of the CoMFA calculations, steric and electrostatic interactions were calculated using an sp3 hybridised carbon atom with a Van der Waals radius of 1.52 and a +1 charge as steric and electrostatic probes, respectively, and a Tripos force field with a distance dependent dielectric constant at all intersections in a regularly spaced grid of two angstroms. The maximal steric and electrostatic energy was determined to be 30 kcal/mol, and this value served as the cut-off. The minimum column filtering was set to 2.0 kcal/mol in order to increase the signal-to-noise ratio. This meant that lattice points with energy fluctuations that were smaller than this threshold were omitted from the analysis.

2.6 Calculation of comparative molecular similarity indices analysis descriptors

An sp3 hybridised carbon probe atom with a radius of one and a +1 charge was used to evaluate the five CoMSIA similarity index fields (steric, electrostatic, hydrophobic, H-bond donor, and H-bond acceptor). These lattice points were located in the same grid region that was used for CoMFA calculations. A Gaussian type that depends on distance was utilised in the region of the molecule that lay between the grid point and each atom. It was decided to use the standard value of 0.3 for the attenuation factor. The minimal value for column filtering was established at 1.0 kcal/mol.

2.7 PLS analysis

The PLS method was used to do the regression analysis. The LOO method was used to do the cross-validation analysis. In this method, one compound is taken out of the dataset and its activity is predicted by using the model made from the rest of the dataset.

The optimal number of components was found using the LOO method, and that number was used in a final analysis that didn't involve cross-validation. The results were then looked at.

The cross-validated correlation coefficient (q2) that led to the best number of components and the lowest SEE was taken into account for further analysis and calculated using the following formula.

$$q^2 = 1 - \frac{\sum\left(Y_{pred} - Y_{exp}\right)^2}{\sum\left(Y_{exp} - Y_{mean}\right)^2}$$

where γpred, γactual and γmean are predicted, actual and mean values of the target property (pIC50), respectively. Equal weights for CoMFA were assigned to steric and electrostatic fields using the CoMFA_STD scaling option. To derive 3D-QSAR models, CoMFA and CoMSIA descriptors were used as an independent variable and pIC_{50} activity value as a dependent variable.

2.8 Predictive coefficient of determination

17 compounds that were left out of the model development process served as a test set for the QSAR models' prediction abilities. These 17 molecules were optimised for geometry and energy minimization, just like the compounds in the training set discussed above. The model created from the training set was used to predict the activity of these molecules. Based on the molecules in the test set, the predictive coefficient of determination (r^2 pred) is determined using the formula

where SD is the sum of the squared deviation bet ween the biological activity of the test set molecules and the mean activity of the training set molecules. Predictive residual sum of square (PRESS) is calculated by taking the difference in predicted and actual activity of the test set molecules. For all conventional analysis (non-cross-validation) the ‘minimum sigma’ standard deviation threshold was set to 2.0 kcal/mol,

3. Results and discussion

3.1 HQSAR analyses

The HQSAR model was developed using 53 structurally unique benzimidazole derivatives and three separate parameters: fragment size, the hologram length, and the fragment type. This was done on a set of benzimidazole derivatives (fragment distinction). In the beginning, a total of 14 HQSAR models were developed employing a variety of fragment distinctions, including A/B, A/B/C, A/B/C/H, A/B/C/Ch, A/B/C/H/Ch, A/C/DA, A/B/C/H/DA, A/B/H, and A/B/H/DA, with fragment sizes ranging from 4–7. Because both hydrogen bond donor and acceptor were included in the models that showed high cross-validated q^2 values, it is possible that hydrogen bond donor and acceptor play a major part in the regulation of the antihypertensive action of benzimidazole derivatives.

Based on the hologram length of 353 and six components, we were able to produce the best HQSAR model **07** (q^2 = 0.983, r^2 =0.991, SEE =0.004) by employing atoms/bonds/connection/hydrogen atoms/donor and acceptor as distinction information (Table 2). To further examine the impact of length of fragment sizes, the best HQSAR model 06 employing A/B/C/H/DA was selected (2–5, 3–6, 4–7, 5–8, 6–9, 7–10 and 8–11). Model 20 with hologram length 257 and six components yielded the most favourable statistical statistics (q^2 = 0.990, r^2 = 0.992, SEE = 0.003) when compared to the other models. According to the findings, a larger fragment size has the potential to contribute to an improvement in the HQSAR model. The key findings are outlined in Table 2.

Table 2. HQSAR analysis for various fragment distinctions using default fragment size (4–7).

S.No.	Components	q^2	r^2	SEE	HL	n
1	A/B	0.976	0.990	0.004	307	6
2	A/B/C	0.970	0.665	0.003	151	6
3	A/B/C/H	0.978	0.984	0.005	353	6
4	A/B/C/Ch	0.991	0.995	0.003	151	6
5	A/B/C/H/Ch	0.977	0.984	0.005	353	6
6	A/C/DA	0.985	0.992	0.003	199	6
7	**A/B/C/H/DA**	**0.983**	**0.991**	**0.004**	**353**	**6**

8	A/B/H	0.976	0.984	0.005	307	6
9	A/B/H/DA	0.976	0.984	0.005	199	6
10	A/B/C/DA	0.978	0.993	0.003	353	6
11	A/B/Ch/DA	0.970	0.985	0.005	401	6
12	A/B/H/Ch	0.979	0.982	0.005	353	6
13	A/B/DA	0.972	0.986	0.005	199	6
14	A/B/Ch	0.977	0.992	0.003	257	6
15	A/B/C/H/Ch/DA	0.975	0.987	0.004	353	6

q^2, cross-validated correlation coefficient; r^2, non-cross-validated coefficient of determination; SEE, standard error of estimate; n, number of statistical components; HL, hologram length; A, atoms; B, bonds; C, connection; H, hydrogen atoms; Ch, chirality; DA, donor and acceptor.

Table 3. HQSAR analysis for various fragment size using the best fragment distinction (atoms/ bonds/connection/hydrogen atoms/donor and acceptor) and all of the 153 odd numbers of hologram lengths from 97 to 401.

S.No.	Components	q^2	r^2	SEE	HL	n
15	2-5	0.975	0.983	0.005	307	6
16	3-6	0.976	0.981	0.005	257	6
17	4-7	0.979	0.984	0.005	353	6
18	5-8	0.980	0.986	0.004	353	6
19	6-9	0.985	0.991	0.004	307	6
20	**7-10**	**0.990**	**0.992**	**0.003**	**257**	**6**
21	8-11	0.981	0.995	0.054	257	6

q^2,cross-validated correlation coefficient; r^2, non-cross-validated coefficient of determination; SEE, standard error of estimate; n, number of statistical components; HL, hologram length; A, atoms; B, bonds; C, connection; H, hydrogen atoms; Ch, chirality; DA, donor and acceptor.

HQSAR provides information about the individual atomic contribution to the biological activity by use of different colour codes. Fragment colours in yellow and green reflect its positive contribution while white-coloured fragments reflect an intermediate contribution. The contribution of different fragments for antihypertensive activity can be explained by compound 6, the most active in the dataset. The fragment contribution map (Figure 2)

showed that the benzimidazole scaffold represented by the green, yellow and white colour code in compound 6 (pIC_{50} = 10) showed its positive contribution to antihypertensive potency.

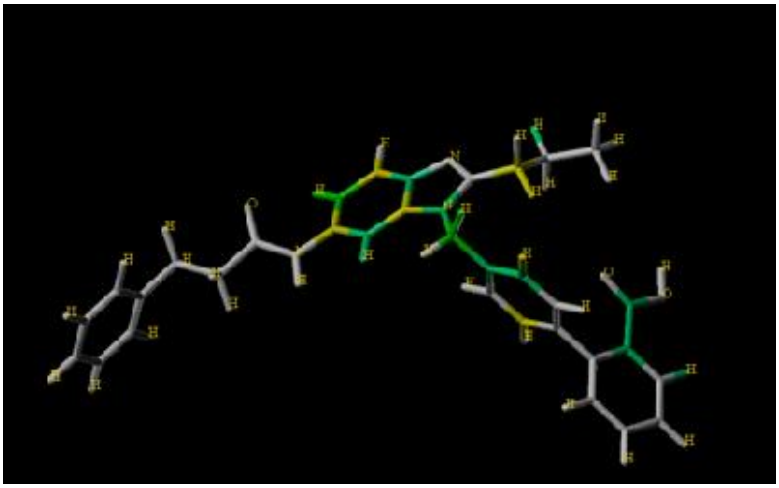

Figure 2. HQSAR contribution map of the most active compound 06.

3.2 Analyses of the CoMFA

The results of PLS analysis showed the cross-validation of the steric and electrostatic CoMFA fields produced a q^2 value of 0.778 with four components, a non-cross-validated r^2 value of 0.996, and a standard error of estimation (SEE) value of 0.0467. The contribution of the electrostatic field is 29.70 percent, whereas the contribution of the steric field is 70.30 percent.

3.3 Analyses of the CoMSIA

There was a total of twelve distinct CoMSIA models produced by utilising a variety of different molecular field combinations. Therefore, the combination of steric (S), electrostatic (E), hydrophobic (H), hydrogen bond donor (D) and hydrogen bond acceptor (A) fields was selected as the best model.

The models that included the combination of steric, electrostatic, hydrophobic, and hydrogen-bond donor and acceptor fields produced the greatest q^2 (0.776) with an optimized four components, and they produced the highest r^2 (0.990) with a standard error of estimation of 0.0466. The respective contributions of steric, electrostatic, hydrophobic, hydrogen-bond donor and acceptor fields were 21.00 percent, 19.00 percent, 16.10 percent, 22.60 percent, and 21.30 percent, respectively. Tables 4 and 5 provide a summary of the statistical parameters used for calculating CoMSIA and CoMFA, respectively. All the results indicate that the CoMSIA model is also fairly predictive.

Table 4. Summary of CoMSIA results.

S.No.	CoMSIA field	q^2	r^2	SEE	n
1	**S/E/H/D/A**	**0.776**	**0.996**	**0.04664**	**4**
2	S/E/H/D	0.716	0.994	0.05513	4
3	S/E/H/A	0.318	0.996	0.04399	4
4	S/H/D/A	0.415	0.995	0.03577	4
5	S/E/D/A	0.402	0.995	0.05002	4
6	E/H/D/A	0.442	0.996	0.04393	4
7	S/E/H	0.23	0.993	0.05687	4
8	S/E/D	0.412	0.992	0.06101	4
9	E/H/D	0.415	0.995	0.04819	4
10	E/H/A	0.352	0.996	0.04405	4
11	S/H/D	0.411	0.996	0.04650	4
12	S/H/A	0.267	0.993	0.06015	4

3.4 Validation of QSAR models

The predictive ability of the HQSAR (r^2 pred = 0.991), CoMFA (r^2 pred = 0.996) and CoMSIA (r^2 pred = 0.996) models were found acceptable and the results are shown in Table 5. However, the statistical result and plot of the experimental and predicted pIC_{50} values of HQSAR, CoMFA and CoMSIA are reported in Table 6 and Figure 4.

Table 5. Summary of HQSAR, CoMFA and CoMSIA models results

Component	**HQSAR**	**CoMFA**	**CoMSIA**
q^2	0.992	0.178	0.776
r^2	0.990	0.996	0.996
r^2_{pred}	9.998	10.00	9.97
N	6	4	4
HL	257	-	-
SEE	-	0.467	0.0466
Steric	-	0.703	0.210

Electrostatic	-	0.297	0.190
Hydrophobic	-	-	0.161
Donor	-	-	0.226
Acceptor	-	-	0.213

q^2,LOO cross-validated correlation coefficient; r^2, non-cross-validated coefficient of determination; r^2 pred, predictive coefficient of determination, number of components used in the PLS analysis; SEE, standard error of estimate; HL, hologram length

CoMFA contour map analysis

In order to view the effects of the field on the target features, the best CoMFA and CoMSIA models are chosen to be used in the construction of the contour maps. All the contours showed the default level of contribution, which was 80% for favourable regions and 20% for unfavourable regions. The only exception to this was the figure of hydrogen bond donor contour maps, which showed 70% and 30% level contributions. The maps showed regions where differences in molecular fields are associated with differences in biological activity. The steric contour maps of the CoMFA are displayed in Figure 3a. The steric interaction is shown by the contours in green and yellow, whereas the electrostatic interaction is shown by the contours in red and blue. A large green contour was found near the substituent group of phenylene position indicating that bulky substituents were preferred in this region and near the carboxylic group (Figure 3a).

A Figure 3b presents the CoMFA electrostatic contour maps for the compounds. On the other hand, the positively charge-favoured regions of the electrostatic contour map are defined by the blue contour, while the negatively charge-favoured regions are shown by the red contour. A blue contour in the CoMFA electrostatic map (Figure 3b) indicates that the presence of an electron-donating group at this position, such as an alkyl group, favours antihypertensive activity and the existence of two red contours indicates that negatively charged groups at this position are favourable for antihypertensive activity.

Figure 3. CoMFA steric/electrostatic contour maps for compound 6:

CoMFA Steric 3a	CoMFA Electrostatic 3b
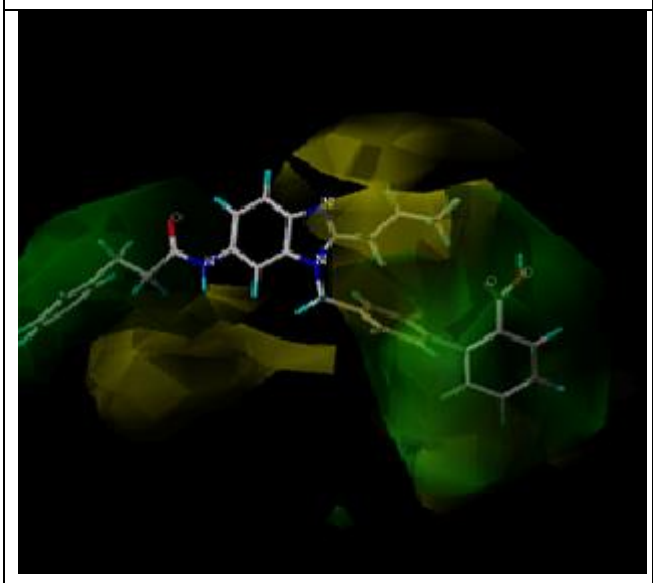	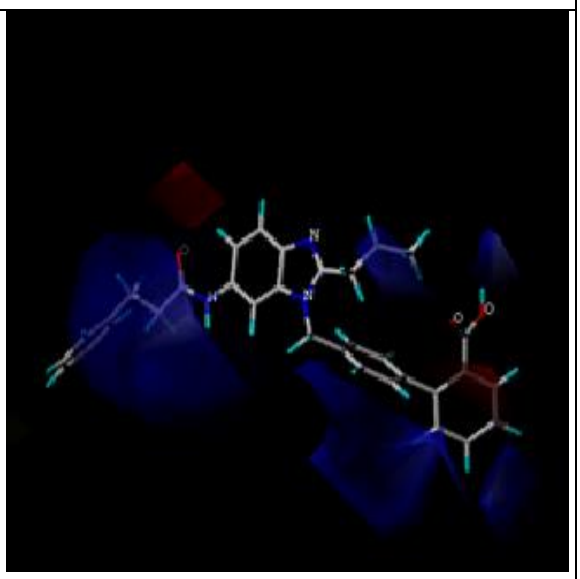

3.5 ***CoMSIA contour map analysis***

In steric and electrostatic CoMSIA study the green colour and blue color is favoured while the yellow and red coloured is disfavoured. (a) In steric fields, green contours show where bulky groups or substituents are needed and more active, while yellow contours show where they are less active. (b) In Electrostatic fields: blue contours close to the phenyl ring indicates the need of electrons with a positive charge are more active and red contours show where electrons with a negative charge are more active. Under the framework of the (c) hydrophobic interaction, the yellow contours and white contours indicate places in which an increase in lipophilicity and hydrophilicity will result in an increase in activity. (d) The H-bond donor contour map. The cyan contour shows areas with higher hydrogen-bond donor group activity. (e) H-bond acceptor contour map; the magenta contour shows places with increased activity of hydrogen-bond acceptor groups.

Figure 4. *CoMSIA contour map* (a) Steric fields:

COMSIA (a) Steric	COMSIA (b) Electrostatic	COMSIA (c) Hydrophobic
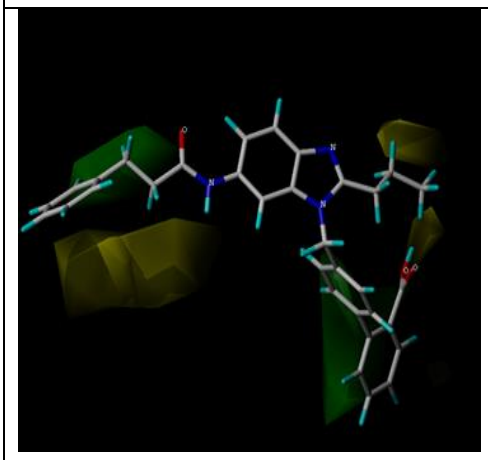	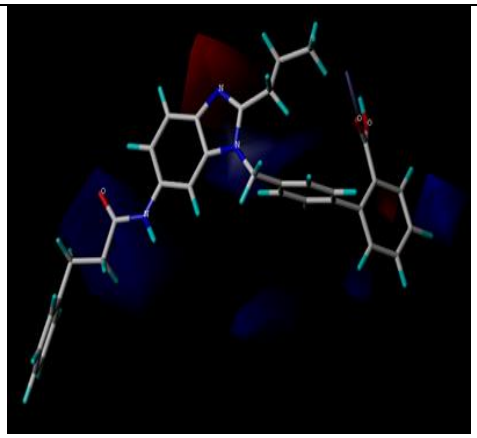	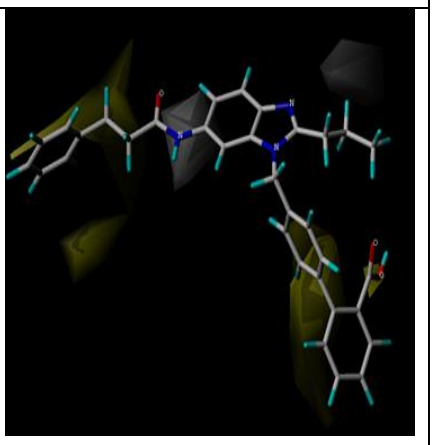

CoMSIA (d) *Donar*	CoMSIA (e) *acceptor*
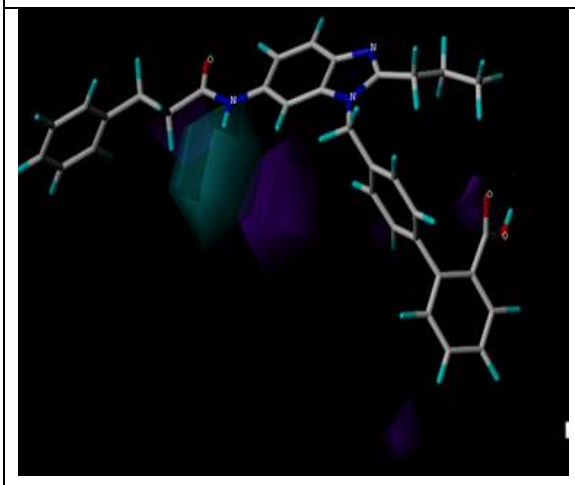	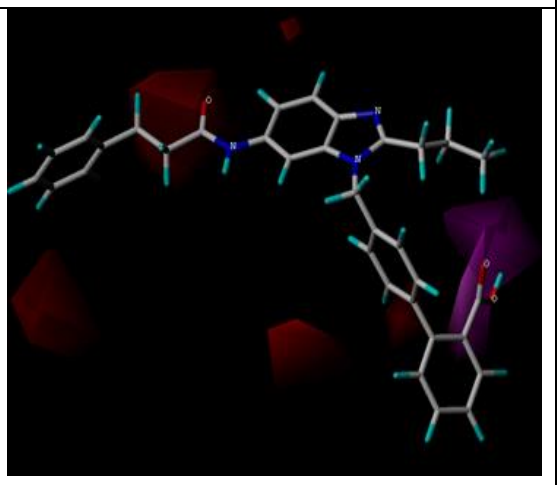

Table 6. Experimental and predicted pIC50 values of training and test set compounds.

Compound	Experimental	HQSAR		COMFA		COMSIA	
		Predicted	Residual	Predicted	Residual	Predicted	Residual
1. *	9.397	9.399	-0.002	9.40	-0.003	9.38	0.017
2.	9.522	9.519	0.003	9.45	0.072	9.21	0.312
3.	8.408	8.410	-0.002	8.40	0.008	8.34	0.068
4.	8.309	8.308	0.001	8.31	-0.001	8.40	-0.091
5.	8.920	8.918	0.002	8.96	-0.04	8.96	-0.04

6. *	10.00	9.998	0.002	10.00	0	9.97	0.03
7. *	9.154	9.149	0.005	9.17	-0.016	9.27	-0.116
8.	7.886	7.885	0.001	7.90	-0.014	7.90	-0.014
9. *	7.698	7.688	0.01	7.70	-0.002	7.77	-0.072
10.	7.408	7.406	0.002	7.44	-0.032	7.38	0.028
11. *	8.522	8.519	0.003	8.44	0.082	8.51	0.012
12.	7.958	7.956	0.002	7.99	-0.032	7.88	0.078
13. *	8.000	8.030	-0.03	8.00	0	7.94	0.06
14. *	8.127	8.124	0.003	8.14	-0.013	8.14	-0.013
15.	8.737	8.728	0.009	8.73	0.007	8.78	-0.043
16.	9.443	9.440	0.003	9.47	-0.027	9.48	-0.037
17.	8.583	8.580	0.003	8.61	-0.027	8.60	-0.017
18. *	7.946	7.942	0.004	7.98	-0.034	7.95	-0.004
19. *	8.083	8.079	0.004	8.11	--0.027	8.08	0.003
20.	7.884	7.879	0.005	7.83	0.054	7.84	0.044
21.	8.424	8.420	0.004	8.50	-0.076	8.51	-0.086
22.	8.651	8.649	0.002	8.51	0.141	8.51	0.141
23.	9.036	9.039	-0.003	9.06	-0.024	9.06	-0.024
24. *	8.469	8.461	0.008	8.47	-0.001	8.47	-0.001
25.	8.449	8.440	0.009	8.36	0.089	8.34	0.106
26.	8.327	8.320	0.007	8.39	-0.063	8.38	-0.053
27.	8.249	8.241	0.008	8.31	-0.061	8.36	-0.111
28. *	8.931	8.929	0.002	8.96	-0.029	8.92	0.011
29.	8.485	8.475	0.01	8.44	0.045	8.44	0.045
30.	8.251	8.244	0.007	8.24	0.011	8.33	-0.079
31.	7.987	7.961	0.026	7.98	0.007	8.02	-0.033
32.	8.397	8.356	0.041	8.33	0.067	8.38	0.017
33.	8.004	7.999	0.005	7.95	0.054	7.97	0.034
34. *	7.917	7.910	0.007	7.92	-0.003	7.92	-0.003
35.	8.275	8.265	0.01	8.34	-0.065	8.33	-0.055
36.	7.978	7.937	0.041	7.98	-0.002	7.93	0.048
37.	7.920	7.919	0.001	7.93	-0.01	7.91	0.01

38.	8.356	8.346	0.010	8.32	0.036	8.34	0.016
39.	7.970	7.965	0.005	8.00	-0.03	7.99	-0.02
40.	7.866	7.860	0.006	7.94	-0.074	7.88	-0.014
41.	8.251	8.240	0.011	8.25	0.001	8.30	-0.049
42.	8.013	8.00	0.013	7.98	0.033	7.96	0.053
43. *	8.148	8.144	0.004	8.19	-0.042	8.12	0.028
44. *	8.136	8.130	0.006	8.03	0.106	8.13	0.006
45.	8.318	8.310	0.008	8.28	0.038	8.27	0.048
46.	8.267	8.260	0.007	8.27	-0.003	8.30	-0.033
47.	8.283	8.234	0.049	8.29	-0.007	8.29	-0.007
48.	9.096	9.088	0.008	9.10	-0.004	9.11	-0.014
49.	8.481	8.422	0.059	8.47	0.011	8.47	0.011
50. *	8.346	8.246	0.1	8.37	-0.024	8.35	-0.004
51. *	8.638	8.630	0.008	8.58	0.058	8.59	0.048
52. *	8.251	8.240	0.011	8.26	-0.009	8.26	0.009

Figure 5. Graph of predicted versus Experimental pIC50 values for the training and test set compounds. (a) HQSAR; (b) CoMFA; (c) CoMSIA.

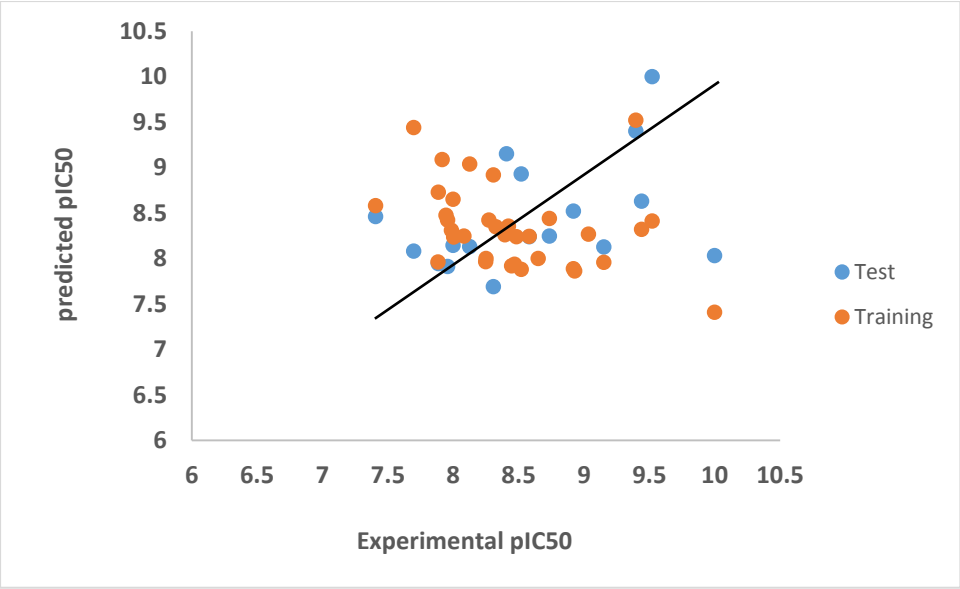

(a) HQSAR

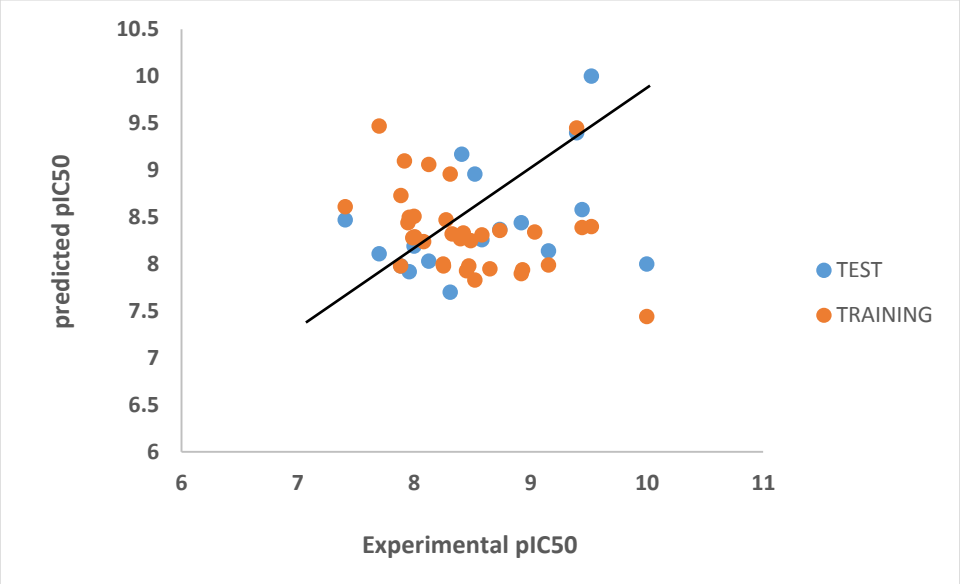

(b) CoMFA

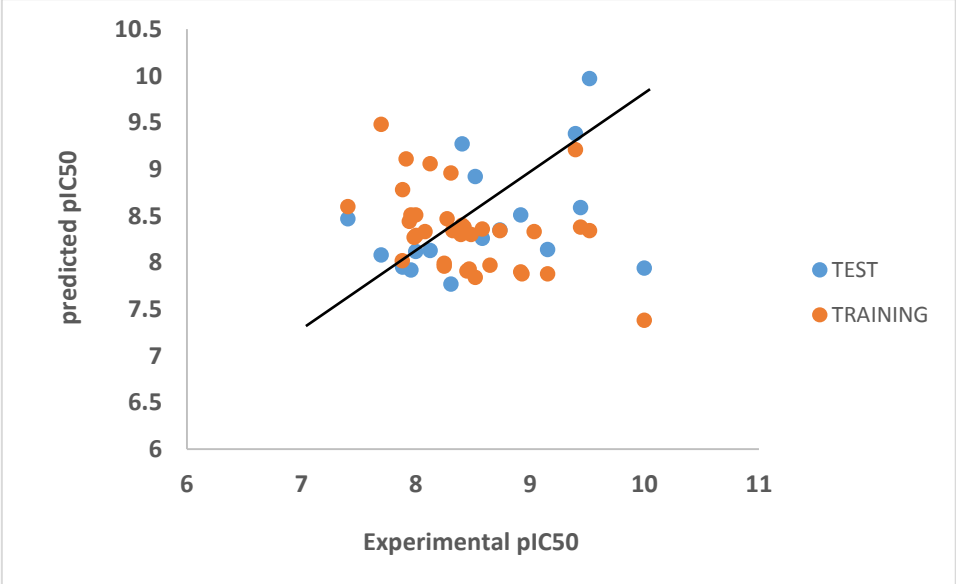

(c) CoMSIA

Conclusion-

In conclusion, we have effectively utilised HQSAR, CoMFA, and CoMSIA approaches to develop highly predictive 2D- and 3D-QSAR models for 52 structurally distinct benzimidazole derivatives. The accuracy of these QSAR models was shown by the strong connection between experimental and predicted activity for test and training set compounds. In addition, the QSAR models were validated using internal LOO cross-validation techniques and external test set techniques. The antihypertensive activity of benzimidazole is

significantly influenced by atoms, bonds, connections, hydrogen atoms, donor and acceptor descriptors, as revealed by HQSAR.

As a result, we using the data derived from the results of the HQSAR fragment contribution map, as well as the CoMFA and CoMSIA contour maps.

The results of CoMFA, CoMSIA and HQSAR provide adequate information to understand the structure–activity relationship and to identify structural features affecting antihypertensive potency.

References-

[1] World Health Organisation, *WHO 2021 World Hypertension Report*. Available at https://www.who.int/southeastasia/news/detail/17-05-2022-world-hypertension-day---measure-your-blood-pressure--control-it--live-longer

[2] Yuan Lu, Yun Wang, Erica S. Spatz, Oyere Onuma,Khurram Nasir,Fatima Rodriguez,Karol E. Watson and Harlan M. Krumholz/; *National Trends and Disparities in Hospitalization for Acute Hypertension Among Medicare Beneficiaries*, Circulation. 2021;144:1683–1693

[3] Jun Zhang, Jin-Liang Wang , Wei-Fa Yu, Zhi-Ming Zhou, Wen-Chang Tao, Yi-Cheng Wang, Wei ZheXue, Di Xua, Li-Ping Hao, Xiao-Feng Han, Fan Fei, Ting Liu, Ai-Hua Liang, "*Nonpeptidic angiotensin II AT1 receptor antagonists derived from 6-substituted aminocarbonyl and acylaminobenzimidazoles"* European Journal of Medicinal Chemistry 69 (2013) 44-54.

[4] Wu Zhuo, Nguyen Thi Phuong Anh, Yi -Jia Yan, Ming -Bao Xia, Yan -Hui Wang, Yan Qiu, Zhi- Long Chen "*Nonpeptidic angiotensin II AT1 receptor antagonists derived from 6-substituted aminocarbonyl benzimidazoles*" European Journal of Medicinal Chemistry 181 (2019) 111553.

[5] Z. Wu, M-B.Xia, D. Bertsetseg, Y-H. Wang, X-L.Bao, W-B.Zhu, Tao-Xu, P-R.Chen, H-S.Tang, Y-J. YAN, Z-L Chen, *Design, Synthesis and biological evalution of novel fluoro-substituted benzimidazole derivatives with anti-hypertension activities*, Bioorganic Chemistry , (2020) 104042.

[6] Weibo Zhu, XiaoluBao, He Ren, Yajing Da, Dan Wa, Fuming Li, Yijia Yan, Li Wang, ZhilongChen, "*N- phenyl indole derivatives as AT1 antagonists with antihypertension activities: Design, synthesis and biological evaluation*" European Journal of Medicinal

Chemistry 115 (2016) 161-178.

[7] Zhuo Wu et al., *Design, Synthesis, and Biological Evaluation of 6-Benzoxazole Benzimidazole Derivatives with Antihypertension Activities*, ACS Med.Chem. Lett. 10, (2019) 40-43.

[8] J. Sainy & R. Sharma, *QSAR analysis of thiolactone derivatives using HQSAR, CoMFA and* CoMSIA SAR and QSAR in Environmental Research, 26 (2015), pp. 873–892,

[9] N. Eswar, B. Webb, M.A. Marti-Renom, M. Madhusudhan, D. Eramian, M.Y. Shen, U. Pieper, and A. Sali, *Comparative protein structure modeling using MODELLER*, Curr. Protoc. Bioinf. 5 (2006), pp. 1–30.

[10] R.D. Cramer III, D.E. Patterson, and J.D. Bunce, *Comparative molecular field analysis (CoMFA):I. Effect of shape on binding of steroids to carrier proteins*, J. Am. Chem. Soc. 110 (1988), pp. 5959–5967.

[11] G. Klebe, U. Abraham, and T. Mietzner, *Molecular similarity indexes in a comparative-analysis (CoMSIA) of drug molecules to correlate and predict their biological activity*, J. Med. Chem. 37 (1994), pp. 4130–4146.

[12] SYBYL-X 2.1, Tripos Inc., St. Louis, MO.

[13] T.L. Moda, C.A. Montanarib, and A.D. Andricopulo, *Hologram QSAR model for the prediction of human oral bioavailability*, *Bioorg*. Med. Chem. 15 (2007), pp. 7738–7745.

[14] Goyal et al., Synthesis And Pharmacological Evaluation Of Some Novel Imidazole Derivatives For Their Potential Anti-Hypertensive Activity, Journal Of Pharmaceutical Technology, Researc And Management, (2013), 1, 69–79.

[15] Liu et al., Design, *Synthesis, And Biological Evaluation Of 1, 2, 4-Triazole Bearing 5-Substituted Biphenyl-2-Sulfonamide Derivatives As Potential Antihypertensive Candidates*, Journal Of Bioorganic & Medicinal Chemistry, (2013), 21, 7742–7751.

[16] Parateet al., *Synthesis and Evaluation of Substituted 1, 2, 4 Triazolinone Derivatives as Novel Angiotensin Ii Receptor Antagonists as Antihypertensive Agents*, Middle-East Journal of Scientific Research, (2013), 17(2), 237-244.

[17] Wubulikasimu et al., *Synthesis And Biological Evaluation Of Novel Benzimidazole Derivatives Bearing A Heterocyclic Ring At 4/5 Position*, Bull. Korean Chem. Soc, (2013), 34(8), 2297-2304.

[18] Kalyankar et al., *Review on Benzimidazole Derivative*, International Journal Of Chemical And Pharmaceutical Sciences, (2012), 3(4), 1-10

[19] A.V.Chobanian, et al., *The Seventh Report of The Joint National Committee on Prevention, Detection, Evaluation, and Treatment of High Blood Pressure, Journal of American Medical Association, (*2003), 289(19), 2560-72.

[20] Anupama A Parate "*Study Of Binding Site For Losartan And Irbesartan As Angiotensin Ii Receptor Antagonists As Antihypertensive Agents"Research Journal Of Pharmaceutical*, Biological And Chemical Sciences,2014, 5(1), 1117-1134.

[21] Vázquez et al., *Synthesis, Vasorelaxant Activity And Antihypertensive Effect Of Benzo [D] Imidazole Derivatives*, Journal Of Bioorganic & Medicinal Chemistry, (2010), 18, 3985–3991.

[22] Sharma et al., *Synthesis and Biological Evaluation Of Some New Benzimidazoles Derivatives 4'-{5-Amino-2-[2-Substituted-Phenylamino)-Phenyl-Methyl]-Benzimidazol-1 Ylmethyl} - Biphenyl-2-Carboxylic Acid: Nonpeptide Angiotensin Ii Receptor Antagonists*, International Journal Of Drug Delivery 2, (2010), 265-277.

[23] Mohamed A.H. Ismail, M. Nabil AboulEnein, Khaled A.M. Abouzid, Dalal A. Abou El Ella, Nasser S.M. Ismail "*ACE inhibitors hypothesis generation for selwctive design, synthesis and biological evaluation of 3- mercapto-2-methyl- propanoyl-pyrrolidine-3 imine derivatives as antihypertensive agents*" European Journal of Medicinal Chemistry 17(2009) 3739-3746

[24] Jin-Liang Wang, Jun Zhang, Zhi-Ming Zhou , Zhi-Huai Li, Wei-ZheXue, Di Xu, Li-Ping Hao, Xiao-Feng Han, Fan Fei, Ting Liu, Ai-Hua Liang, "*Design, synthesis and biological evaluation of 6-substituted aminocarbonylbenzimidazole derivatives as nonpeptidic angiotensin II AT1 receptor antagonists*" European Journal of Medicinal Chemistry; 49 (2012); 183-190.

[25] Kalyankar et al., *Review on Benzimidazole Derivative*, International Journal Of Chemical And Pharmaceutical Sciences, (2012), 3(4), 1-10